DALTON

Palladium(0)–tetracyanoethylene complexes of diphosphines and a dipyridine with large bite angles, and their crystal structures §

Mirko Kranenburg,[a] Johannes G. P. Delis,[a] Paul C. J. Kamer,[a] Piet W. N. M. van Leeuwen,*[,a] Kees Vrieze,[a] Nora Veldman,[b] Anthony L. Spek,†[,b] Kees Goubitz‡[,c] and Jan Fraanje[c]

[a] *J. H. van't Hoff Research Institute, Department of Inorganic Chemistry, University of Amsterdam, Nieuwe Achtergracht 166, 1018 WV Amsterdam, The Netherlands*
[b] *Bijvoet Center for Biomolecular Research, Laboratorium voor Kristal-en Structuurchemie, University Utrecht, Padualaan 8, 3584 CH Utrecht, The Netherlands*
[c] *Amsterdam Institute for Molecular Studies, Department of Crystallography, University of Amsterdam, Nieuwe Achtergracht 166, 1018 WV Amsterdam, The Netherlands*

Complexes of Pd(tcne) (tcne = tetracyanoethylene) containing bidentate ligands with large bite angles, bis[2-(diphenylphosphino)phenyl] ether (L^1), 4,6-bis(diphenylphosphino)-10,10-dimethyl-10*H*-dibenzo[*b*,*e*][1,4]oxasiline(L^2), 4.6-bis(diphenylphosphino)-2,8-dimethylphenoxathiine (L^3), 4,5-bis(diphenylphosphino)-9,9-dimethylxanthene (L^4) and *trans*-5,6-bis(2-pyridyl)bicyclo[2.2.1]hept-2-ene (L^6), were prepared and characterised. The compound 4,6-bis(diphenylphosphino)dibenzo[*b*,*d*]furan (L^5) did not form chelating palladium complexes, owing to its large natural bite angle of 138°. The crystal structures of L^6, $[PdL^1(tcne)]\cdot 2.5CH_2Cl_2$ **1**, $[PdL^2(tcne)]\cdot 4CH_2Cl_2$ **2**, $[PdL^4(tcne)]\cdot 2CH_2Cl_2$ **4** and $[PdL^6(tcne)]$ **5** have been determined. The similarity of electronic effects induced by the free diphosphines was demonstrated by MOPAC calculations. The geometries of the ligands, however, were most accurately predicted by molecular mechanics (MM2) calculations for the diphosphines, and MNDO for L^6. The largest P–Pd–P angle in the zerovalent palladium complexes was found to be 104.6°. A further increase in the natural bite angle of the ligand results in elongation of the Pd–P bond length in the complex rather than enlargement of the P–Pd–P bite angle. The ligand L^6 assumed a bite angle of 99.5(2)° in complex **5**, which is considerably smaller than its calculated value of 117°.

Olefin complexes of zerovalent palladium of the form PdL_2(olefin) have not been studied as extensively as the analogous nickel and platinum compounds. In part this may be due to the relative instability of complexes such as $[Pd(PPh_3)_2(C_2H_4)]$ compared to those of Ni and Pt.[1–3] The importance of zerovalent palladium complexes in various homogeneously catalysed reactions[2,4–6] justifies a detailed investigation into the structural features of these compounds, especially since the importance of steric and electronic factors in catalyst activity is well recognised.[7]

The available crystal structures of Pd^0(diimine)(olefin) complexes show a very narrow range of N–Pd–N angles, due to the rigid *cis*-fixating characteristics of the ligands 2,2′-bipyridine [N–Pd–N 76.3(4), 76.4(4)°][8] and 1,2-bis[2,6-bis(isopropylphenyl)imino]acenaphthene, $C_{12}H_6[N(C_6H_3Pr^i_2\text{-}2,6)]_2$-1,2 [N–Pd–N 77.78(19)°].[9] In crystal structures of Pd^0(diphosphine)(olefin) complexes the observed P–Pd–P angles vary enormously, depending on steric demands: 115.1(1)° for $[Pd(PMe_3)_2(\eta^2\text{-}CH_2{=}CC_4Me_4)]$,[10] 109.7(2)° for $[Pd(PPh_3)_2(C_{60})]$,[11] 109.3(1)° for $[Pd(PPh_3)_2(C_3H_4)]$,[12] 106.4° for [Pd(diop)(C_2H_4)],[13] 88.9((1)° for $[Pd\{(C_6H_{11})_2PCH_2CH_2P(C_6H_{11})_2\}(\eta^2\text{-}CH_2{=}CHCH{=}CH_2)]$,[14] and 84.78(5)° for [Pd(dppe)(dba)][15] (dppe = $Ph_2PCH_2CH_2PPh_2$, dba = dibenzylideneacetone). Theoretical studies indicate that the P–M–P angle in the metal fragment will be between 94 and 110°. Hofmann *et al.*[16] studied the geometrical characteristics for platinum diphosphine fragments using extended-Hückel calculations. They found an energy minimum for $[Pt(PH_3)_2(C_2H_4)]$ at a P–Pt–P angle of 110°. Sakaki and Ieki[17] calculated a P–Pt–P angle of 103° for $[Pt(PH_3)_2(Si_2H_4)]$ and $[Pt(PH_3)_2(SiH_2CH_2)]$, and 107° for $[Pt(PH_3)_2(C_2H_4)]$. These calculations were performed at the *ab initio* level. A recent quasi-relativistic density-functional study by Ziegler and co-workers[18] reports calculated bite angles of 110.8–117.1° for $[Pd(PH_3)_2(C_2H_4)]$, 109.0–109.9° for $[Ni(PH_3)_2(C_2H_4)]$ and 104.9–110.6° for $[Pt(PH_3)_2(C_2H_4)]$, depending on whether or not relativistic effects are taken into account. These theoretical calculations focused mainly on the olefinic part of the complex and paid little attention to the P–M–P angle.

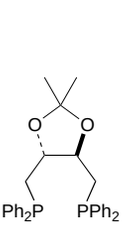

diop

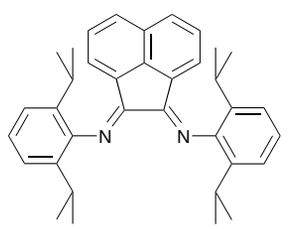

$C_{12}H_6[N(C_6H_3Pr^i_2\text{-}2,6)]_2$-1,2

Recently, we developed a new group of diphosphines L^1–L^5 designed to enforce large bite angles (*i.e.* larger than 90°), which are, unlike traditional diphosphines such as 1,2-bis-(diphenylphosphino)ethane (dppe), ideally suitable to stabilise the bite angles found in trigonal and tetrahedral geometries.[19] These compounds are based on heterocyclic xanthene-like aromatics, and by varying the bridge in the 10 position of the backbone we were able to induce variations in the bite angle.

The natural bite angle (β_n) and flexibility range were calculated by molecular modelling, using an augmented MM2[20] force field. The natural bite angle is defined as the preferred chelation angle determined only by ligand-backbone con-

† For correspondence pertaining to crystallographic studies on complexes **1**, **2** and **4**.
‡ For correspondence pertaining to crystallographic studies on L^6 and complex **5**.
§ *Non-SI units employed*: cal = 4.184 J, dyn = 10^{-5} N, au ≈ 1.60×10^{-19} C.

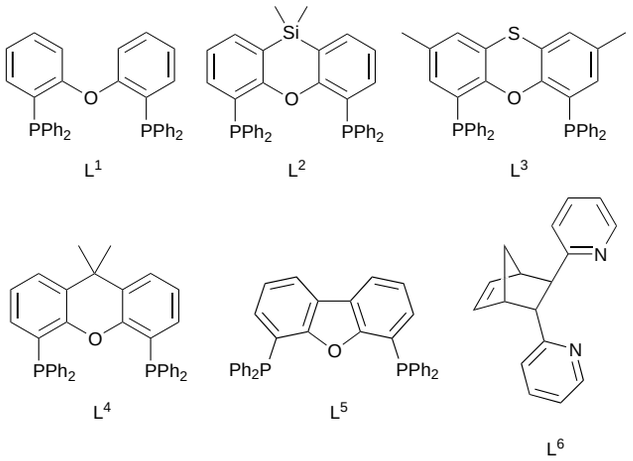

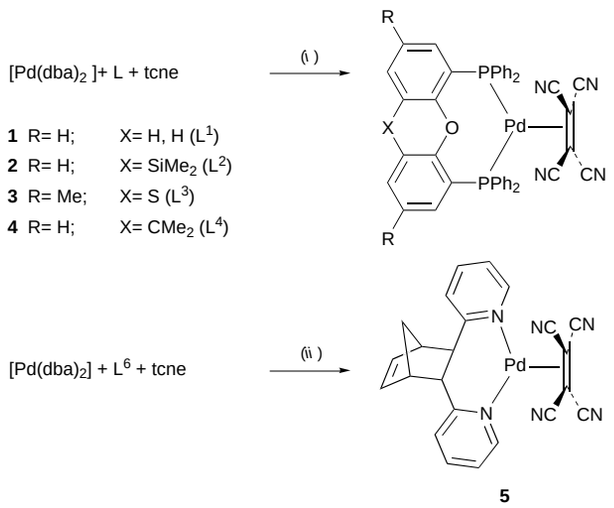

5

Scheme 1 (*i*) C_6H_6, room temperature (r.t.); (*ii*) toluene, r.t.

straints and not by metal valence angles. The flexibility range is defined as the accessible range of bite angles within less than 3 kcal mol^{-1} excess strain energy from the calculated natural bite angle.[21] According to our calculations, these ligands have natural bite angles varying from 100 to 138°, and a flexibility range of *ca.* 35° (for palladium complexes). Recent studies on hydroformylation,[19,22] hydrocyanation,[23] reductive carbonylation[24] and reductive elimination[25] have shown that the bite angle has a strong influence on catalyst selectivity. The electronic effects of the variations in the backbone are expected to be small and the steric sizes of the substituents on phosphorus are identical in all ligands.[7] Therefore the interaction between the geometrical demands of the ligand and those of the metal centre can be studied.

Previous experiments with either mono- or bi-dentate compounds with smaller, constrained, natural bite angles have never produced evidence for the preferred valence angle in palladium(0) complexes. The application of electronically and sterically similar diphosphines with natural bite angles ranging from 100 to 138° will, however, allow a detailed investigation of this preferred valence angle.

Results and Discussion

Synthesis

In addition to the aforementioned diphosphines, we synthesized a new bidentate dipyridyl compound with a rigid norbornene backbone. Chiral 5,6-bis(2-pyridyl)bicyclo[2.2.1]hept-2-ene (L^6) has been prepared by a Diels–Alder cycloaddition of cyclopentadiene and *trans*-1,2-bis(2-pyridyl)ethylene. A racemic mixture of two enantiomers was obtained, which was used without separation. Most bidentate nitrogen ligands such as α-diimines have bite angles of about 78°.[9,26] The relatively rigid L^6 was designed to enforce large bite angles analogously to the phosphines mentioned. For this compound we calculated a natural bite angle of 117.5°, and a flexibility range of 26° (from 105 to 131°). The product has been characterised by ^1H, ^{13}C and ^1H–^1H COSY (correlation) NMR spectroscopy and elemental analysis. Crystals (of one enantiomer) suitable for crystallographic structure determination were grown from a solution of the product in pentane at 243 K.

We prepared palladium–tcne complexes (tcne = tetracyanoethylene) of L^1–L^4 and L^6 in high yield by reaction of $[Pd(dba)_2]$ with tcne and L in benzene or toluene (Scheme 1).[9] After decanting and washing with diethyl ether to remove the dba, the crude product was dissolved in CH_2Cl_2 and filtered (in air) to remove metallic palladium. The yellow complexes are very stable in air, although during melting-point determinations a continuous darkening of the powder was observed upon heating. With the exception of [PdL^3(tcne)] **3**, crystals suitable for X-ray crystallographic structure determination were obtained by either concentrating a CH_2Cl_2 solution under a gentle stream of N_2 or slow diffusion of pentane into a CH_2Cl_2 solution.

Attempts to synthesize [PdL^5(tcne)] did not yield any characterisable complex. This again indicates that the bite angle of L^5 (β_n = 138°, see Table 4) is too large for successful co-ordination, as was already apparent from its performance in catalytic reactions[19,23] and attempts to prepare other transition-metal complexes.[19,27]

Electronic influence and geometry of the ligands

The geometry of the diphosphines changes little on co-ordination to Pd, as can be concluded from comparison of the crystal structure of L^4 (ref. 19) (see Fig. 7) and that of complex **4** (see Fig. 6). When the calculated structures of L^1 and L^2 are compared to those of complexes **1** and **2**, respectively, similar results are obtained. Comparison of chelational properties of different ligands, based on strictly steric arguments such as the cone angle[7] and the bite angle, is of course only valid when electronic influences are kept constant. Since the Pd(tcne) fragment is the same for all complexes, the only difference that can arise is that from the ligands. We calculated the partial charges in the free phosphines to quantify the possible electronic differences induced by them. These net atomic charges were determined by MOPAC[28] calculations. Starting geometries for the calculations were that of the crystal structure for L^4 and the geometry as produced by computational methods for the other diphosphine ligands. The exact input geometry of the molecules proved to be of great importance for the results of the calculations. When the partial charges for L^4 as calculated for the X-ray geometry and the MM2 geometry are compared significant differences are observed. The results obtained for different compounds are therefore only comparable when the same method is used for the determination of the geometries. Since crystal structures are not available for all the diphosphines, we investigated which method is most accurate in the prediction of the ligand geometry. As sample ligands L^4 and L^6 were used, since these are the only ones of this series for which crystal structures are available.

The computational methods tested were molecular mechanics (using the MM2 force field)[20] and the semiempirical MOPAC-AM1,[29] PM3[30] and MNDO[31] methods. The input structures for the geometry optimisation were the crystal structures. The results are presented in Figs. 1 and 2.

The MOPAC calculations of the diphosphine show a large overestimation of the planarity of the backbone compared to the crystal structure. Especially the AM1 and MNDO calculations, which produce a backbone which is almost planar. The PM3 calculated structure is somewhat better in that respect, but

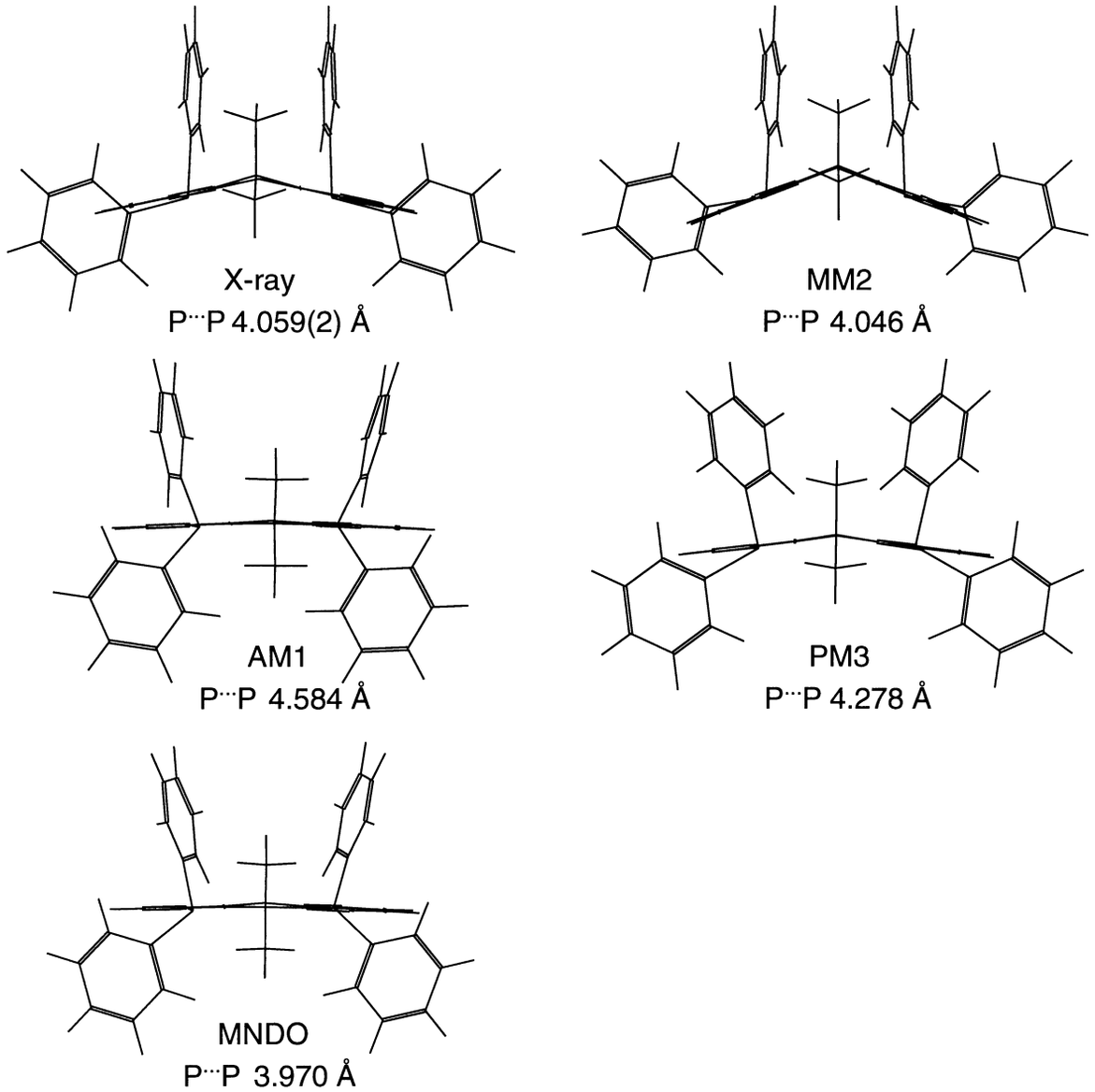

Fig. 1 Geometry of compound L^4 as calculated with MM2, MNDO, PM3 and AM1 methods compared to the crystal structure

in this the P · · · P distance is too large [4.278 compared to 4.059(2) Å in the crystal structure]. The π-stacking interaction between the phenyl rings of the diphenylphosphine moieties is held responsible for the observed bending of the backbone in L^4. When this interaction is hindered, as in 4,6-bis{bi[4-(diethylaminomethyl)phenyl]phosphino}-9,9-dimethylxanthene where the (diphenylphosphino)phenyl groups of L^4 are substituted with a *p*-(diethylamino)methyl group, the xanthene backbone is almost flat [a dihedral of 176.7(2) Å].[32] This planarity of the backbone is also observed in the crystal structure of 10,10-dimethylphenoxasiline, the backbone of L^2.[33] The ring system in 10,10-dimethylphenoxasiline is almost planar (dihedral angle between the two phenyl rings 175.6°). This planarity is almost the same as that observed in the 9,9-dimethylxanthene backbone L^7.

The importance of attractive interactions between π systems is well recognised,[34] but semiempirical SCF (self-consistent field) techniques have not been very successful in describing these interactions.[35,36] None of the MOPAC calculations reproduces the π-stacking interaction accurately,[37] and it can be concluded that an important factor determining the overall geometry of these compounds is not taken into account. More advanced methods do offer the possibility to reproduce these interactions.[35,38,39]

The MM2 calculated structure showed an underestimation of the planarity of the backbone of L^4 and the resulting geometry is somewhat similar to that in the [PdL^4(tcne)] complex (see below). The P · · · P distance calculated for L^4 is very close to the observed distance [4.046 Å, compared to 4.059(2) Å in the crystal structure], and the orientation of the diphenylphosphine moieties (caused by π-stacking of the phenyl rings) is identical to that of the crystal structure. It can be concluded that the overall geometry is best predicted by MM2 calculations. This is of course also favoured from a practical point of view, since MM calculations require much less computing time than do MOPAC calculations. In addition, MM can be augmented more easily for use in specific problems (such as natural bite-angle calculations).

For compound L^6 the results of all the calculations are in much better agreement with the crystal structure. In Fig. 2 the calculated structures are superimposed on the crystal structure. The differences are most evident when the orientation of the pyridyl rings is evaluated, but this is not very important since the energy barrier for rotation is very small. More importantly, MOPAC, and especially AM1 and MNDO, gives a more accurate description of the C–C–H angles around the sp^3-carbon atoms in the norbornene backbone of L^6 than does MM2. Deviations in these angles can have large influences on the cal-

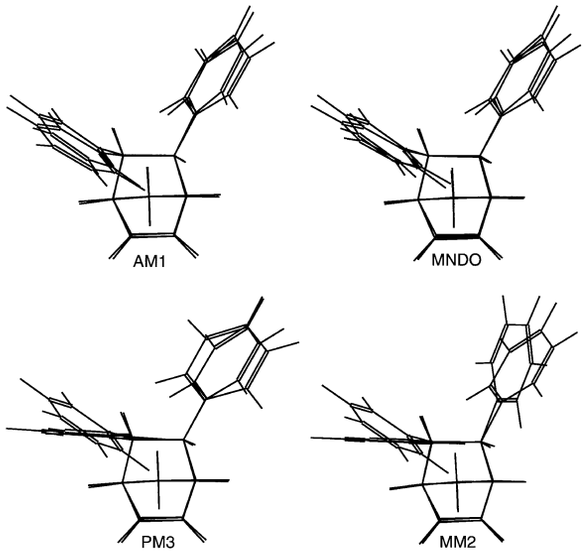

Fig. 2 Geometry of compound L[6] as calculated in Fig. 1 superimposed on the crystal structure

Table 1 Net atomic charges as calculated using MOPAC-PM3

	Charge (au)	
Compound	P(1)	P(2)
L[1]	0.7721	0.7262
L[2]	0.7242	0.7243
L[3]	0.7031	0.7301
L[4]	0.7272	0.7272
	0.7522 *	
L[5]	0.7240	0.7522 *
		0.7283

Geometry as produced by MM2 calculations. * Geometry as in the crystal structure.

culated bite angle. For L[6], π-stacking interactions have no influence on the overall geometry and in this case the MOPAC calculations produce better results than does MM2. It can be concluded that MNDO is the most accurate method for the prediction of the ligand geometry of L[6].

The ligand geometry was predicted best by MM2 calculations for the diphosphines, and therefore the geometries obtained by MM2 were used for calculation of the partial charge on the phosphorus atoms. The calculations (summarised in Table 1) show that these partial charges are nearly the same for the whole range of compounds. It can therefore be concluded that there is little or no electronic influence of the changes we have made in the ligand backbones on the phosphorus-atom donor properties. The absolute values calculated using different MOPAC methods differ significantly, but the results of each method are similar for the range of compounds (0.72 for PM3, 0.67 for AM1 and 0.43 for MNDO). The results reported here for the phosphines are those obtained from PM3 calculations since this method gives more accurate results for molecules containing phosphorus.[30,40]

Crystal structures

The molecular structures and adopted numbering schemes are presented in Figs. 3–6 and 8. Selected bond distances, angles, and torsion angles are compiled in Tables 2, 3 and 6.

The structure of free L[6] (Fig. 3) shows the norbornene fragment with the two pyridyl groups in a *trans* position which makes the molecule chiral. The angles around the sp^3-carbon atoms C(4) and C(5) are distorted due to the strain induced by

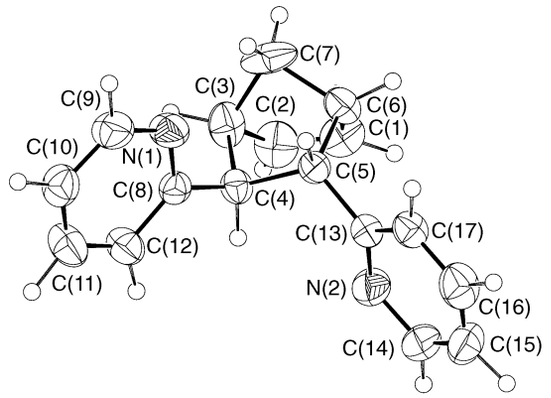

Fig. 3 An ORTEP[41] representation of the crystal structure of compound L[6] drawn at the 50% probability level

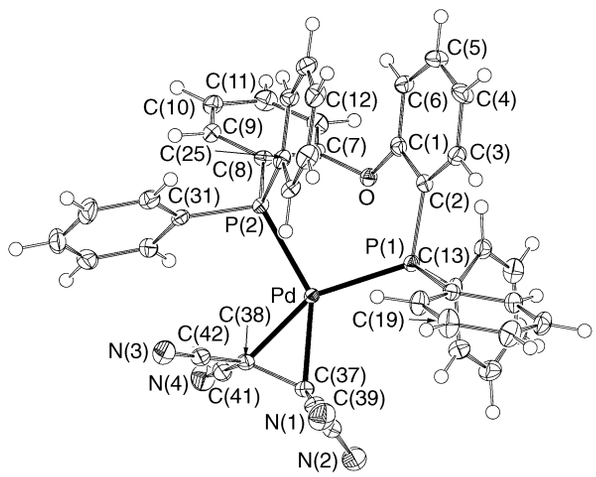

Fig. 4 An ORTEP representation of the crystal structure of complex **1** drawn at the 50% probability level. Solvent molecules are omitted for clarity

the norbornene ring. The dihedral angle between the two pyridyl rings is 80.3(1)°.

In the structures of the diphosphine complexes the palladium centres are surrounded by atoms P(1), P(2), C(37) and C(38). The co-ordination is trigonal planar (Y shaped) as expected for zerovalent complexes of the type ML_2(alkene) (M = Pd or Pt).[42] Comparison of the geometry of **4** (Fig. 6) and that of uncomplexed L[4] (ref. 19) (Fig. 7) shows that the geometry of the ligand has changed very little upon complexation (see below).

The geometries of the diphosphine fragments are determined strongly by π–π stacking interactions. In complex **1** one of the rings [C(1)–C(6)] of the backbone is nearly parallel to a PPh_2 phenyl ring [C(25)–C(30)]. The angle between the rings is 20.16(16)°, whereas in **2** and **4** two phenyl rings of the diphenylphosphine moieties [C(13)–C(19) and C(25)–C(30)] are almost parallel, with respective angles between the planes of 19.3(4) and 23.5(3)°.

The alkene bond distances C(37)–C(38) are 1.485(4) Å in complex **1**, 1.508(11) Å in **2**, and 1.475(7) Å in **4**, all longer than that in the free alkene (1.34 Å)[42] as a result of the expected back donation from the metal.

The tcne fragment is no longer planar, the cyano groups being bent away from the plane which is caused by a rehybridisation towards sp^3 around the olefinic C atom upon co-ordination to the palladium. A method to quantify this non-planarity of the co-ordinated olefin has been introduced by Ittel and Ibers,[42] involving the angles α and β. The angle α is that between the normals to the planes defined by the substituent groups; β and β′ are the angles between the normals to the planes between the olefin bond and the aforementioned plane

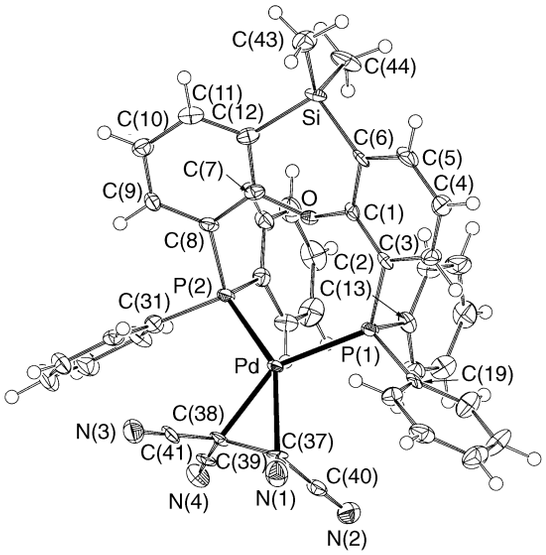

Fig. 5 An ORTEP representation of the crystal structure of complex **2**. Details as in Fig. 4

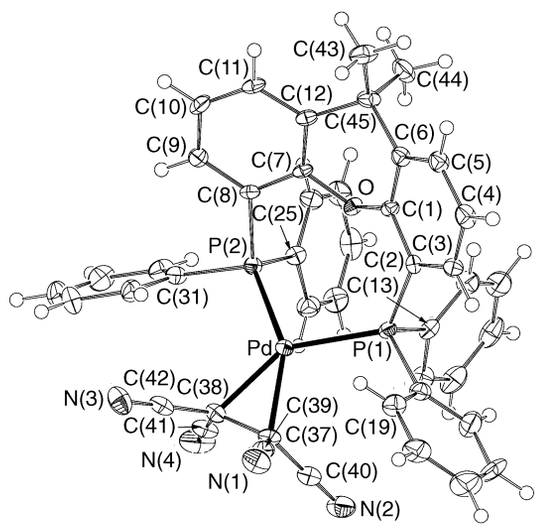

Fig. 6 An ORTEP representation of the crystal structure of complex **4**. Details as in Fig. 4

normals (Scheme 2). As bending back of the substituents occurs, α becomes larger than 0° and β becomes smaller than 90°. The α and β values for complexes **1**, **2**, **4** and **5** are presented in Table 4.

The average Pd–C (alkene) distance, 2.11 Å, is comparable to those found in $[Pd\{(C_6H_{11})_2CH_2CH_2P(C_6H_{11})_2\}(\eta^2\text{-}CH_2{=}CH\text{-}CH{=}CH_2)]$[14] [2.130(3) Å].

The average Pd–P distances are in the same range as those found in other palladium diphosphine systems: 2.332 Å in complexes **1** and **2**, and 2.354 Å in **4**. The probable cause of this slightly longer bond distance in **4** becomes clear when the P···P distances and the P–Pd–P bite angles are compared (see Table 5). The observed bite angle for **1** [P(1)–Pd–P(2) 101.46(3)°] is significantly smaller than those for **2** [104.28(7)] and **4** [104.64(5)°], as expected from our MM calculations. The angles for **2** and **4** are almost the same, however, which is not expected since the calculated natural bite angles for the ligands are significantly different.

When we compare the observed P···P distances in the crystal structures it is seen that for complex **4** this distance is larger than that for **2**. In our model a larger P···P distance results in a larger P–M–P bite angle (natural bite angle), since the same P–Pd bond length is used in all MM calculations and metal valence angles are not taken into account. The larger P···P

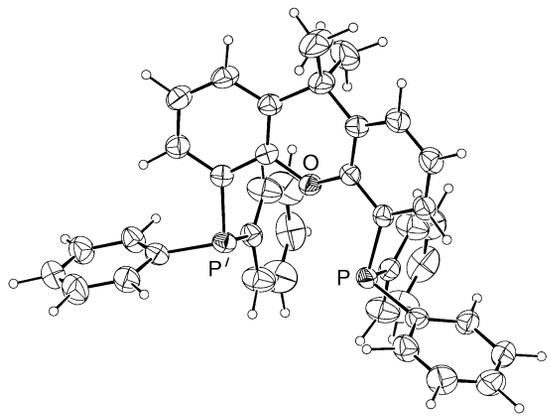

Fig. 7 An ORTEP representation of the crystal structure of uncomplexed L^4 (ref. 19) drawn at the 30% probability level

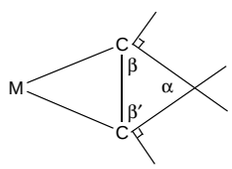

Scheme 2 Illustration of angles α, β and β′

distance is compensated by an elongation of the Pd–P bond in **4**. Owing to this elongation the resulting P–Pd–P bond angle is only 104.64(5)°. The fact that the Pd–P bond lengths differ so much in structures that are chemically so much alike as **2** and **4** seems to indicate that the palladium valence angle has reached an upper limit. The ligand L^4 can chelate successfully, yielding a stable complex, but only by elongation of the P–Pd bond length. Thus, while L^4 has a natural bite angle of 109°, the above results show that the Pd(tcne) fragment clearly prefers, for electronic reasons, a smaller P–Pd–P angle. Previous experiments with either mono- or bi-dentate compounds with smaller, constrained, natural bite angles have never produced evidence for the preferred valence angle in such complexes.

We modelled a hypothetical $[PdL^5(tcne)]$ complex with the observed maximum P–Pd–P angle of 104.64°. For the ligand L^5 the MM2 energy is 11.8 kcal mol^{-1} higher and the heat of formation calculated using PM3 is 30.2 kcal mol^{-1} higher than that for unconstrained L^5. We can therefore conclude that the adjustment in geometry for L^5 in order to support successful co-ordination costs so much energy that chelation is very unlikely.

We observed that due to electronic effects diphosphines with natural bite angles near 110° adopt much smaller bite angles in Pd(diphosphine)(tcne) complexes. Using L^6 we will show that this effect is even larger for dinitrogen ligands. The structure of complex **5** shows the bidentate co-ordination of L^6 to the trigonal-planar palladium centre with η^2-co-ordinated tcne (see Fig. 8).

The bond lengths Pd–N(2) of 2.142(5) Å and Pd–N(1) of 2.100(4) Å are in the range observed for crystal structures of other Pd(N–N)(η^2-alkene) complexes.[9,43,44] The α and β values (see above) for **5** are presented in Table 4. The Pd–C (alkene) distances of 2.029(5) and 2.016(4) Å are significantly shorter than those in the palladium phosphine complexes (2.11 Å) but comparable with those of other Pd(N–N)(η^2-alkene) complexes.[9,43,44] The alkene bond distance C(18)–C(19) of 1.476(7) Å is similar to those in both palladium phosphine and other Pd(N–N)(η^2-alkene) complexes, while the N(1)–Pd–N(2) bite angle of 99.5(2)° is significantly larger than those in other Pd(N–N)(η^2-alkene) complexes (*ca.* 78°).[9] The calculated natural bite angle (β_n = 117°) for L^6 is larger than its observed bite angle [N–Pd–N 99.5(2)°]. To accommodate this latter bite angle, the Pd atom is not co-ordinated in the plane of the pyridyl groups, but it is bent out of the planes at 11.9(1)°

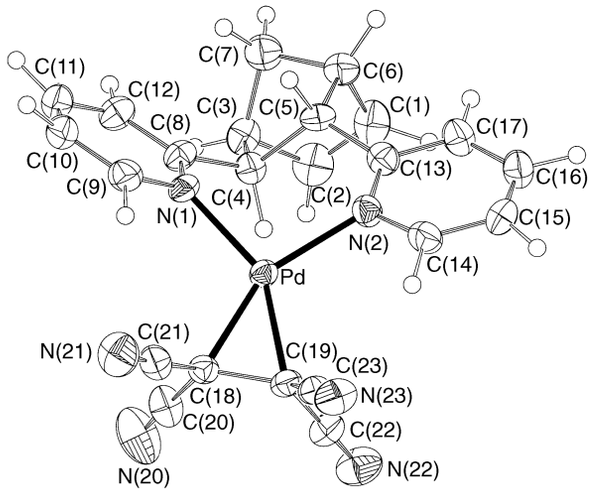

Fig. 8 An ORTEP representation of the crystal structure of complex **5** drawn at the 50% probability level

[C(11)···N(1)–Pd 164.6(3) and C(16)···N(2)–Pd 167.7(3)°]. The MM calculations do not *a priori* take into account a deviation out of the plane and hence the calculated β_n is much larger. The heat of formation of the AM1-optimised geometry of the ligand with a N···N distance locked at 3.238 Å (the observed N–N distance in the crystal structure) is 3.9 kcal mol^{-1} higher than that of unco-ordinated L[6]. The difference in MM2 energy is only 0.5 kcal mol^{-1} higher. These differences in energy are very small, which indicates that the compound is well capable of adjusting its geometry towards the demands invoked by the palladium centre.

When the out of plane deviation of the Pd is included in the calculations, the natural bite angle decreases to 106.5°. Although much smaller than the original β_n of 117°, this value is still significantly higher than the observed N–Pd–N angle, indicating a large strain on this angle. Hence for pyridine ligands the preference for a small valence angle (<100°) is even more pronounced than that found in the phosphine complexes. The compound L[6] can easily accommodate angles between 105 and 120° and yet the electronic preference of palladium dictates a N–Pd–N angle of only 99.5(2)°. These observations are in line with molecular orbital calculations, which have shown that stronger σ donors induce smaller D–M–D angles in Y-shaped D_2MA complexes (D = donor, A = acceptor).[45]

It is difficult to compare the quasi-relativistic density-functional calculations by Ziegler and co-workers[18] on [Pd(PH$_3$)$_2$(C$_2$H$_4$)] with the thus observed 'maximum' bite angle in Pd^0(tcne) of 105°. Comparison of the P–M–P angles in the crystal structures of [Ni(PPh$_3$)$_2$(C$_2$H$_4$)] [P–Ni–P 110.5(2)°],[46] [Pt(PPh$_3$)$_2${C$_2$(CN)$_4$}] [P–Pt–P 101.4(3)°],[47] [Pt(PPh$_3$)$_2$(C$_2$Cl$_4$)] [P–Pt–P 100.6(2)°][48] and [Pt(PPh$_3$)$_2$(C$_2$H$_4$)] [P–Pt–P 111.6(1)°][49] shows that the influence of the d^{10} metal on the geometry is much less than that of the alkene. Replacing ethene in [Pt(PPh$_3$)$_2$(C$_2$H$_4$)] by a more electron-withdrawing alkene such as tcne reduces the bite angle by *ca.* 10°, whereas replacement of platinum by nickel in [M(PPh$_3$)$_2$(C$_2$H$_4$)] causes a decrease in the P–M–P angle of only 1°. Comparison of the P–Pd–P angle in **2** [104.28(7)] and **4** [104.64(5)°] to the P–Pt–P angle in [Pt(PPh$_3$)$_2${C$_2$(CN)$_4$}] [101.4(3)°], however, shows that the L[4]-type ligands do induce a significant enlargement of the P–M–P angle.

Conclusion

We started this investigation by designing ligands with large natural bite angles (110–120°) in order to stabilise trigonal co-ordination. The present results show that for the stabilisation of Pd^0 bound to the strong acceptor tcne the preferred bite angle is much smaller. Using diphosphines with natural bite angles ranging from 100 to 109°, the largest P–Pd–P angle found is 104.64(5)°. A larger P···P distance in the ligand results in slight elongation of the Pd–P bond length rather than enlargement of the P–Pd–P bite angle. Co-ordination of the better σ-donating ligand L[6], with a β_n of 117.5°, reduces the N–Pd–N bite angle even further, to 99.5(2)°. To accommodate this small bite angle, the palladium centre is bent out of the planes of the pyridyl rings by 11.9(1)°.

Table 2 Selected bond lengths (Å), bond/valence angles (°) and torsion angles (°) for compound L[6] with estimated standard deviations (e.s.d.s) in parentheses

N(1)–C(8)	1.336(4)	C(1)–C(2)	1.255(6)
N(1)–C(9)	1.344(5)	C(4)–C(5)	1.551(4)
N(2)–C(13)	1.375(4)	C(4)–C(8)	1.513(4)
N(2)–C(14)	1.375(4)	C(5)–C(13)	1.507(4)
C(8)–N(1)–C(9)	117.8(4)	C(5)–C(4)–C(8)	115.1(2)
C(13)–N(2)–C(14)	117.2(3)	C(4)–C(5)–C(13)	116.4(3)
C(2)–C(1)–C(6)	110.7(4)	C(3)–C(7)–C(6)	91.2(3)
C(1)–C(2)–C(3)	107.7(3)		
C(9)–N(1)–C(8)–C(12)	−1.8(4)		
C(9)–N(1)–C(8)–C(4)	177.7(3)		
C(14)–N(2)–C(13)–C(17)	0.3(5)		
C(14)–N(2)–C(13)–C(5)	179.7(3)		
C(5)–C(4)–C(8)–N(1)	47.8(3)		
C(8)–C(4)–C(5)–C(13)	103.3(3)		
C(4)–C(5)–C(13)–N(2)	39.4(4)		

Experimental

Computational details

All calculations were performed using CAChe WorkSystem software[50] on an Apple Power Macintosh 950 equipped with two CAChe CXP coprocessors. The molecular mechanics calculations were performed using the MM2[20] force field. The block-diagonal Newton–Raphson method was employed for optimisation. Natural bite angle calculations were performed using a method similar to that described by Casey and Whiteker,[21] using a Pd–P bond length of 2.332 Å and a Pd–N bond length of 2.120 Å.

The flexibility range was calculated by fixing the L–Pd–L angle (L = P or N) at a given value, minimising the constrained molecule with molecular mechanics and dynamics. The excess strain energy was calculated by normalising the energy obtained for this strained molecule with that of the structure obtained by the natural bite-angle calculation. This procedure was repeated at intervals of 5°.

The geometry optimisations of the different techniques were compared by minimising the crystal structures of compounds of L[4] (ref. 19) and L[6]. Geometry optimisation by MOPAC-PM3,[30] AM1,[29,40,51,52] and MNDO[31,53–55] calculations (CAChe-MOPAC, version 94.10; derived from MOPAC, version 6.00[28]), were performed using eigenvector following. Partial charges were determined by performing SCF energy calculations using MOPAC. Input structures were those produced by X-ray diffraction analysis for L[4] and L[6], and the geometries as produced by MM2 calculations for all diphosphines. The gradient was minimised using eigenvector folllowing. As a base for our calculations on a hypothetical [PdL^5(tcne)] complex with the observed maximum P–Pd–P angle of 104.64° we took the crystal structure of **4**, locked the Pd(tcne) fragment and the P–Pd–P angle, and assigned a bond-stretch force constant of 0 mdyn $Å^{-1}$ for the P–Pd bond. The structure obtained by this procedure has Pd–P bond lengths of *ca.* 2.66 Å and a P···P distance of 4.213 Å. To evaluate the strain on the diphosphine ligand caused by this forced chelation we calculated the MM2 energy and the heat of formation (PM3). the MM2 energy for L^5 optimised with a P···P distance locked at 4.213 Å is 11.8

Table 3 Selected bond lengths (Å), bond/valence angles (°) and torsion angles (°) for complexes **1**, **2** and **4** with e.s.d.s in parentheses

	1	**2**	**4**		**1**	**2**	**4**
Pd–P(1)	2.3420(10)	2.3375(19)	2.3561(13)	P(2)–C(31)	1.821(3)	1.830(8)	1.828(5)
Pd–P(2)	2.3227(9)	2.3262(19)	2.3515(13)	Si/C(45)*–C(6)		1.848(7)	1.527(7)
Pd–C(37)	2.124(4)	2.127(7)	2.110(5)	Si/C(45)*–C(12)		1.870(8)	1.535(7)
Pd–C(38)	2.092(4)	2.101(7)	2.111(5)	Si/C(45)*–C(43)		1.853(8)	1.528(8)
P(1)–C(2)	1.814(4)	1.827(7)	1.822(5)	Si/C(45)*–C(44)		1.840(9)	1.545(6)
P(1)–C(13)	1.824(3)	1.819(8)	1.815(5)	O–C(1)	1.393(4)	1.391(9)	1.391(6)
P(1)–C(19)	1.807(3)	1.820(7)	1.818(5)	O–C(7)	1.392(3)	1.389(9)	1.380(5)
P(2)–C(8)	1.830(3)	1.826(7)	1.824(5)	C(37)–C(38)	1.485(4)	1.508(11)	1.475(7)
P(2)–C(25)	1.818(3)	1.816(8)	1.814(5)				
P(1)–Pd–P(2)	101.46(3)	104.28(7)	104.64(5)	C(12)–C(45)/Si*–C(43)		113.4(3)	111.4(4)
P(1)–Pd–C(37)	111.97(8)	107.2(2)	105.38(4)	C(12)–C(45)/Si*–C(44)		108.4(4)	107.4(4)
P(1)–Pd–C(38)	152.97(8)	148.4(2)	145.57(14)	C(43)–C(45)/Si*–C(44)		112.7(4)	110.4(4)
P(2)–Pd–C(37)	145.17(8)	146.8(2)	147.47(15)	C(1)–O–C(7)	117.2(2)	121.5(5)	113.4(4)
P(2)–Pd–C(38)	105.52(8)	105.4(2)	107.23(14)	Pd–C(37)–C(39)	117.4(2)	118.7(5)	109.4(3)
C(37)–Pd–C(38)	41.24(11)	41.8(3)	40.92(19)	Pd–C(37)–C(40)	113.0(2)	110.2(5)	118.8(4)
Pd–P(1)–C(2)	117.35(10)	121.9(3)	121.64(12)	Pd–C(37)–C(38)	68.21(19)	68.2(4)	69.6(3)
Pd–P(1)–C(13)	112.75(11)	112.6(3)	110.76(16)	Pd–C(38)–C(37)	70.5(2)	70.1(4)	69.5(3)
Pd–P(1)–C(19)	112.46(12)	109.1(2)	110.42(17)	Pd–C(38)–C(41)	111.0(2)	115.4(5)	119.6(4)
C(2)–P(1)–C(13)	105.04(15)	105.3(3)	105.6(2)	Pd–C(38)–C(42)	116.3(2)	111.3(5)	109.1(3)
C(2)–P(1)–C(19)	102.97(15)	101.2(3)	101.8(2)	C(39)–C(37)–C(40)	115.0(3)	116.9(7)	115.6(4)
C(13)–P(1)–C(19)	105.08(13)	104.9(3)	105.2(2)	C(39)–C(37)–C(38)	118.3(2)	116.3(6)	119.1(5)
Pd–P(2)–C(8)	120.03(9)	120.2(3)	117.75(17)	C(40)–C(37)–C(38)	116.8(3)	117.5(6)	116.2(4)
Pd–P(2)–C(25)	110.29(10)	113.6(3)	114.22(17)	C(37)–C(38)–C(41)	117.9(2)	115.8(6)	117.0(4)
Pd–P(2)–C(31)	110.67(11)	109.3(3)	112.25(16)	C(37)–C(38)–C(42)	119.6(2)	118.5(6)	118.9(5)
C(8)–P(2)–C(25)	107.95(16)	104.4(3)	105.8(2)	C(41)–C(38)–C(42)	113.9(3)	117.0(7)	114.9(5)
C(8)–P(2)–C(31)	102.46(14)	103.8(3)	102.5(2)	N(1)–C(39)–C(37)	178.7(4)	178.2(8)	179.5(6)
C(25)–P(2)–C(31)	104.10(14)	104.1(4)	102.6(2)	N(2)–C(40)–C(37)	178.3(4)	178.5(8)	117.9(6)
C(6)–C(45)/Si*–C(12)		97.9(3)	106.4(4)	N(3)–C(41)–C(38)	178.5(4)	117.6(8)	178.7(5)
C(6)–C(45)/Si*–C(43)		109.5(4)	112.4(4)	N(4)–C(42)–C(38)	179.0(3)	177.7(8)	178.8(6)
C(6)–C(45)/Si*–C(44)		113.8(3)	108.7(4)				
P(2)–Pd–P(1)–C(2)	3.77(11)	62.8(3)	62.96(18)	C(38)–Pd–P(2)–C(31)	7.81(12)	1.0(4)	5.3(2)
P(2)–Pd–P(1)–C(13)	−118.48(12)	−63.8(3)	−61.88(16)	P(1)–Pd–C(37)–C(38)	−175.53(12)	−172.4(4)	−171.4(2)
P(2)–Pd–P(1)–C(19)	122.93(10)	−179.9(3)	−178.04(19)	P(1)–Pd–C(37)–C(39)	−63.9(2)	78.6(6)	−56.6(4)
C(37)–Pd–P(1)–C(2)	−166.24(13)	−127.9(4)	−129.7(2)	P(1)–Pd–C(37)–C(40)	73.5(2)	−60.0(5)	79.2(4)
C(37)–Pd–P(1)–C(13)	71.51(14)	105.4(3)	105.5(2)	P(2)–Pd–C(37)–C(38)	21.8(2)	−11.7(6)	−14.6(4)
C(37)–Pd–P(1)–C(19)	−47.09(13)	−10.7(3)	−10.7(2)	P(2)–Pd–C(37)–C(39)	133.42(19)	−120.7(5)	100.2(4)
C(38)–Pd–P(1)–C(2)	−172.73(19)	−137.6(5)	−139.7(3)	P(2)–Pd–C(37)–C(40)	−89.1(3)	100.8(6)	−124.1(4)
C(38)–Pd–P(1)–C(13)	65.0(2)	95.7(5)	95.4(3)	C(38)–Pd–C(37)–C(39)	111.6(3)	−109.0(7)	114.8(5)
C(38)–Pd–P(1)–C(19)	−53.6(2)	−20.4(5)	−20.7(3)	C(38)–Pd–C(37)–C(40)	−110.9(3)	112.4(7)	−109.5(5)
P(1)–Pd–P(2)–C(8)	70.49(13)	−70.2(3)	−69.23(19)	P(1)–Pd–C(38)–C(37)	9.1(3)	14.0(6)	14.8(4)
P(1)–Pd–P(2)–C(25)	−55.88(13)	54.4(3)	55.8(2)	P(1)–Pd–C(38)–C(41)	−104.2(2)	123.8(5)	125.0(3)
P(1)–Pd–P(2)–C(31)	−170.54(10)	170.1(3)	172.12(18)	P(1)–Pd–C(38)–C(42)	123.4(2)	−99.8(6)	−99.7(4)
C(37)–Pd–P(2)–C(8)	−125.86(18)	−128.8(5)	133.9(3)	P(2)–Pd–C(38)–C(37)	−167.30(13)	173.4(4)	171.8(2)
C(37)–Pd–P(2)–C(25)	107.77(18)	−106.7(5)	−101.1(3)	P(2)–Pd–C(38)–C(41)	79.32(19)	−76.8(6)	−77.9(4)
C(37)–Pd–P(2)–C(31)	−6.89(17)	9.1(5)	15.3(3)	P(2)–Pd–C(38)–C(42)	−53.1(2)	59.7(5)	57.3(4)
C(38)–Pd–P(2)–C(8)	−111.16(15)	120.7(3)	124.0(2)	C(37)–Pd–C(38)–C(41)	−113.4(2)	109.8(7)	110.2(5)
C(38)–Pd–P(2)–C(25)	122.47(14)	−114.7(3)	−111.0(2)	C(37)–Pd–C(38)–C(42)	114.2(3)	−113.7(7)	−114.6(5)

* Si in complex **2**, C(45) in **4**.

Table 4 The non-planarity of the olefin

Compound	α/°	β/°	β′/°
1	55.0(4)	61.0(4)	64.0(4)
2	58.1(9)	61.5(9)	60.4(9)
4	60.9(6)	59.1(6)	60.0(6)
5	59.3(8)	60.8(6)	59.9(5)

kcal mol^{-1} higher than unconstrained L[5]. The PM3 calculations on the MM2-optimised structures showed a difference in heat of formation of 30.2 kcal mol^{-1}.

Synthesis

All preparations were carried out under an atmosphere of purified nitrogen using standard Schlenk techniques. Solvents were carefully dried and freshly distilled prior to use. Benzene was distilled from sodium–benzophenone, dichloromethane from CaH_2. Tetracyanoethylene, cyclopentadiene and 1,2-dipyridylethene was obtained from Aldrich and used as received. The diphosphines[19] and $[Pd(dba)_2]$[56] were prepared as published earlier.

Proton (300), ^{13}C (75.5) and ^{31}P NMR spectra (121.5 MHz, referenced to external 85% H_3PO_4) were recorded on a Bruker AMX-300 spectrometer. Numbering as in the crystal structure was taken for the description of the NMR data for compounds L[6] and **5**. Infrared spectra were obtained on a Nicolet 510 or a Bio-Rad FTS-7 Fourier-transform spectrometer. Melting-point determinations were performed on a Gallenkamp MFB-595 apparatus. Elemental analyses were performed at Dornis and Kolbe, Mülheim a.d. Ruhr, Germany.

***trans*-5,6-Bis(2-pyridyl)bicyclo[2.2.1]hept-2-ene (L[6]).** Aluminium chloride (1.97 g, 14.7 mmol), 1,2-bis(2-pyridyl)ethylene (2.7 g, 14.7 mmol) and freshly cracked cyclopentadiene (3.0 cm^3, 36.8 mmol) were heated in toluene (60 cm^3) at 383 K. After 22 h the reaction mixture was cooled, poured onto ice and a 3 mol dm^{-3} NaOH solution (100 cm^3) in water was added. The aqueous layer was extracted twice with CH_2Cl_2 (100 cm^3). The combined organic layers were dried with Mg_2SO_4. The solvent was evaporated and the residual solid placed on a column with neutral Al_2O_3. Elution with a mixture of diethyl ether–hexane (1:9) yielded the product, which was recrystallised from hex-

Table 5 Calculated and observed L–Pd–L angles (°) and L···L distances (Å) (L = P or N)

Complex	Ligand (L)	Calc. β_n [a]	Calc. distance [b]	Angle in complex	Distance in complex	Distance in free L
1	L^1	100.5	3.582	101.46(3)	3.611	3.594 [b]
2	L^2	104.5	3.686	104.28(7)	3.682	3.899 [b]
3	L^3	105.4	3.711	—	—	3.963 [b]
4	L^4	108.8	3.793	104.64(5)	3.726	4.059(2) [19]
	L^5	137.8	4.392	—	—	5.401 [b]
5	L^6	117.5	*c*	99.5(2)	3.238(6)	*c*

[a] See text. [b] Calculated by MM2. [c] Depends on the orientation of the pyridyl rings.

Table 6 Selected bond lengths (Å), angles (°) and torsion angles (°) for complex **5** with e.s.d.s in parentheses

Pd–N(1)	2.100(4)	N(21)–C(21)	1.133(8)	N(1)–C(9)	1.357(6)	C(18)–C(20)	1.453(7)
Pd–N(2)	2.142(5)	N(22)–C(22)	1.151(8)	N(2)–C(13)	1.359(7)	C(18)–C(21)	1.452(8)
Pd–C(18)	2.029(5)	N(23)–C(23)	1.144(8)	N(2)–C(14)	1.348(7)	C(19)–C(22)	1.435(7)
Pd–C(19)	2.062(5)	C(1)–C(2)	1.352(9)	N(20)–C(20)	1.130(9)	C(19)–C(23)	1.446(8)
N(1)–C(8)	1.345(7)	C(18)–C(19)	1.476(7)				
N(1)–Pd–N(2)	99.49(15)	C(13)–C(17)–C(16)	120.5(5)	Pd–N(1)–C(9)	118.3(3)	Pd–C(19)–C(18)	67.7(3)
N(1)–Pd–C(18)	107.2(2)	Pd–C(18)–C(19)	70.0(3)	Pd–N(2)–C(13)	128.6(3)	Pd–C(19)–C(22)	115.3(4)
N(1)–Pd–C(19)	149.4(2)	Pd–C(18)–C(20)	115.7(3)	Pd–N(2)–C(14)	112.2(3)	Pd–C(19)–C(23)	114.9(3)
N(2)–Pd–C(18)	153.3(2)	Pd–C(18)–C(21)	113.6(4)	C(2)–C(1)–C(6)	107.9(6)	C(18)–C(19)–C(22)	119.8(5)
N(2)–Pd–C(19)	111.1(2)	C(19)–C(18)–C(20)	117.5(5)	C(1)–C(2)–C(3)	106.2(6)	C(18)–C(19)–C(23)	117.4(4)
C(18)–Pd–C(19)	42.3(2)	C(19)–C(18)–C(21)	118.6(4)	C(3)–C(7)–C(6)	94.0(4)	C(22)–C(19)–C(23)	113.9(4)
Pd–N(1)–C(8)	122.4(3)	C(20)–C(18)–C(21)	114.1(4)				

N(2)–Pd–N(1)–C(8)	61.5(4)	C(19)–Pd–C(18)–C(21)	113.4(4)
N(2)–Pd–N(1)–C(9)	−130.7(4)	N(1)–Pd–C(19)–C(18)	4.4(5)
C(18)–Pd–N(1)–C(8)	−116.5(4)	N(1)–Pd–C(19)–C(22)	118.0(4)
C(18)–Pd–N(1)–C(9)	51.3(4)	N(1)–Pd–C(19)–C(23)	−106.6(4)
C(19)–Pd–N(1)–C(8)	−119.6(4)	N(2)–Pd–C(19)–C(18)	−176.7(3)
C(19)–Pd–N(1)–C(9)	48.2(5)	N(2)–Pd–C(19)–C(22)	−63.2(4)
N(1)–Pd–N(2)–C(13)	−38.3(5)	N(2)–Pd–C(19)–C(23)	72.3(4)
N(1)–Pd–N(2)–C(14)	152.3(4)	C(18)–Pd–C(19)–C(22)	113.6(5)
C(18)–Pd–N(2)–C(13)	137.5(5)	C(18)–Pd–C(19)–C(23)	−111.0(5)
C(18)–Pd–N(2)–C(14)	−32.0(6)	Pd–N(1)–C(8)–C(4)	−16.9(6)
C(19)–Pd–N(2)–C(13)	142.3(5)	Pd–N(1)–C(8)–C(12)	164.8(4)
C(19)–Pd–N(2)–C(14)	−27.1(4)	Pd–N(2)–C(13)–C(5)	21.9(7)
N(1)–Pd–C(18)–C(19)	−177.7(3)	Pd–N(2)–C(13)–C(17)	−164.9(4)
N(1)–Pd–C(18)–C(20)	70.6(4)	C(14)–N(2)–C(13)–C(5)	−169.2(5)
N(1)–Pd–C(18)–C(21)	−64.3(4)	C(14)–N(2)–C(13)–C(17)	4.1(8)
N(2)–Pd–C(18)–C(19)	6.8(5)	Pd–N(2)–C(14)–C(15)	167.0(5)
N(2)–Pd–C(18)–C(20)	−105.0(5)	C(13)–N(2)–C(14)–C(15)	−3.7(8)
N(2)–Pd–C(18)–C(21)	120.1(5)	C(8)–N(4)–C(5)–C(13)	108.7(5)
C(19)–Pd–C(18)–C(20)	−111.7(5)		

anes at 233 K. Yield: 1.05 g (4.23 mmol, 28.6%). Crystals suitable for X-ray diffraction were grown from a solution of the product in pentane at 243 K. NMR ($CDCl_3$): δ ^{1}H, 8.53, 8.46 [dd, 2 H, ^3J = 4.8, ^4J = 1.7, H(9), H(14)], 7.06–6.99 [m, 2 H, H(10), H(15)], 7.53, 7.49 [m, 2 H, H(11), H(16)], 7.28, 7.18 [d, 2H, ^3J = 7.9, H(12), H(17)], 6.41 [dd, 1 H, ^3J = 5.6, 3.1, H(1)], 5.98 [dd, 1 H, ^3J = 5.6, 2.7, H(2)], 4.09 [dd, 1 H, ^3J = 5.1, 3.6, H(4)], 3.39 [dd, 1 H, ^3J = 5.3, 3.7, H(5)], 3.36 [s, 1 H, H(3)], 3.07 [s, 1 H, H(6)], 2.17 [d, 1 H, ^3J = 8.3, H(7)], 1.55 [d, 1 H, ^3J = 8.3 Hz, H(7)]; ^{13}C, δ 164.5, 163.9 [C(8), C(13)], 149.5, 149.1 [C(9), C(14)], 138.3, 136.6 [C(11), C(16)], 136.2, 136.0 [C(1), C(2)], 123.8, 122.9 [C(12), C(17)], 121.5, 121.4 [C(10), C(15)], 52.9, 52.4, 50.7, 49.0 [C(3)–C(6)], 47.7 [C(7)]. (Found: C, 82.25; H, 6.45; N, 11.35. Calc. for $C_{17}H_{16}N_2$: C, 82.2; H, 6.5; N, 11.3%).

[PdL^1(tcne)] 1. The complex [Pd(dba)$_2$] (0.200 g, 0.348 mmol), tetracyanoethylene (0.049 g, 0.383 mmol) and L^1 (0.206 g, 0.383 mmol) were dissolved in benzene (40 cm^3). The reaction mixture was stirred for 16 h during which a yellow precipitate formed. The reaction mixture was decanted and washed with ether until the washings were colourless. The crude product was dissolved in CH_2Cl_2 and filtered over paper (in air) to remove metallic palladium. The solvent was removed *in vacuo*. Yield of yellow powder: 0.198 g (0.251 mmol, 72%). Crystals suitable for X-ray diffraction were grown by leading a gentle stream of N_2 through a solution in CH_2Cl_2. NMR ($CDCl_3$): ^{1}H, δ 6–8 (aryl); ^{31}P-{^{1}H}, δ 14.49. IR (ν_{CN}, CH_2Cl_2): 2219 cm^{-1}. M.p. >573 K (decomposes, darkens upon heating).

[PdL^2(tcne)] 2. This compound was prepared by a procedure similar to that described for **1** using [Pd(dba)$_2$] (0.200 g, 0.348 mmol) tcne (0.049 g, 0.383 mmol) and L^2 (0.228 g, 0.383 mmol). Yield of yellow powder: 0.252 g (0.299 mmol, 86%). Crystals suitable for X-ray diffraction were grown by leading a gentle stream of N_2 through a solution in CH_2Cl_2. NMR ($CDCl_3$): ^{1}H, δ 0.642 (br s, 6 H, CH_3), 6.85 (2 H, aryl), 7.16–7.37 (22 H, aryl) and 7.771 (apparent br d, 2 H); ^{31}P-{^{1}H}, δ 7.17. IR (ν_{CN}, CH_2Cl_2): 2219 cm^{-1}. M.p. >573 K (decomposes, darkens upon heating).

[PdL^3(tcne)] 3. This compound was prepared by a procedure similar to that described for **1** using [Pd(dba)$_2$] (0.200 g, 0.348 mmol), tcne (0.049 g, 0.383 mmol) and L^3 (0.228 g, 0.383 mmol). Yield of yellow powder: 0.256 g (0.303 mmol, 87%). NMR ($CDCl_3$): ^{1}H, δ 2.17 (s, CH_3), 6.36 (m, 2 H) and 7.22–7.42 (aryl); ^{31}P-{^{1}H}, δ 7.86. IR (ν_{CN}, CH_2Cl_2): 2219 cm^{-1}. M.p. >573 K (decomposes, darkens upon heating).

[PdL^4(tcne)] 4. This compound was prepared by a procedure similar to that described for **1** using [Pd(dba)$_2$] (0.250 g, 0.435

Table 7 Crystal and refinement data for compounds L^6, **1**, **2**, **4** and **5**

	L^6	**1**	**2**	**4**	**5**
Empirical formula	$C_{17}H_{16}N_2$	$C_{42}H_{28}N_4OP_2Pd\cdot 2.5CH_2Cl_2$	$C_{44}H_{32}N_4OP_2PdSi\cdot 4CH_2Cl_2$	$C_{45}H_{32}N_4OP_2Pd\cdot 2CH_2Cl_2$	$C_{23}H_{16}N_6Pd$
M	248.33	985.41	1168.94	983.01	482.84
Crystal system	Triclinic	Triclinic	Monoclinic	Triclinic	Monoclinic
Space group	$P\bar{1}$ (no. 2)	$P\bar{1}$ (no. 2)	$P2_1/c$ (no. 14)	$P\bar{1}$ (no. 2)	$P2_1/c$ (no. 14)
a/Å	8.3899(8)	12.1157(14)	12.7587(9)	11.8514(7)	9.1090
b/Å	8.9889(9)	13.2623(10)	37.326(2)	12.0742(7)	13.4340
c/Å	9.5220(1)	14.4684(13)	10.9225(9)	18.0974(10)	17.0910
α/°	86.82(1)	79.440(7)		94.757(5)	
β/°	78.04(1)	72.059(9)	100.394(4)	105.937(5)	104.30(2)
γ/°	70.53(1)	75.588(9)		116.033(4)	
U/Å^3	662.3(2)	2127.8(4)	5116.3(6)	2174.6(2)	2026.63
Z	2	2	4	2	4
D_c/g cm^{-3}	1.245	1.538	1.518	1.501	1.582
F(000)	264	994	2360	996	968
μ/cm^{-1}	5.35 (Cu-Kα)	8.6 (Mo-Kα)	9.1 (Mo-Kα)	7.9 (Mo-Kα)	77.28 (Cu-Kα)
Crystal size/mm	0.40 × 0.50 × 0.60	0.20 × 0.20 × 0.57	0.20 × 0.50 × 0.63	0.13 × 0.25 × 0.25	0.25 × 0.40 × 0.50
T/K	253	150	150	150	293
θ_{min}, θ_{max}/°	2.6, 75	1.5, 27.5	1.1, 27.5	1.2, 27.5	2.5, 75
λ/Å	1.5418 (Cu-Kα)	0.710 73 (Mo-Kα)	0.710 73 (Mo-Kα)	0.710 73 (Mo-Kα)	1.5418 (Cu-Kα)
Scan type	ω–2θ	ω	ω	ω–2θ	ω–2θ
Δω/°	1.2 + 0.15 tan θ	0.77 + 0.35 tan θ	1.00 + 0.35 tan θ	0.50 + 0.35 tan θ	1.2 + 0.15 tan θ
Linear decay (%)	None	4	10	2	None
Ranges h, k, l	−10 to 0, −11 to 10, −11 to 11	−14 to 15, −16 to 17, 0–18	−16 to 11, 0–48, −13 to 14	−15 to 13, 0–15, −23 to 23	−10 to 10, 0–15, 0–20
Total data	2702	10 137	14 067	10 470	3443
Total unique data	2702	97 510	11 715	9996	3443
Observed data	2516[$I > 2.5\sigma(I)$]	7575[$I > 2\sigma(I)$]	11 636[$I > 2\sigma(I)$]	6518[$I > 2\sigma(I)$]	3013[$I > 2.5\sigma(I)$]
Absorption correction range	—	—	—	—	0.79, 1.39
No. refined parameters	237	507	588	541	336
R [a]	0.077	0.0423	0.0722	0.0594	0.037
$wR2$ [b]		0.0930	0.1753	0.1120	
R'	0.093				0.059
Goodness of fit	—	1.02	1.06	0.98	—
w^{-1} [d]	7.1 + F_o + 0.0034F_o^2	$\sigma^2(F_o^2)$ + 0.0403P^2 + 0.6873P	$\sigma^2(F_o^2)$ + 0.0410P^2 + 14.95P	$\sigma^2(F_o^2)$ + 0.0372P^2	8.7 + F_o + 0.0119F_o^2
$(\Delta/\sigma)_{av}$, $(\Delta/\sigma)_{max}$	−, 0.46	0.001, 0000	0.000, 0.000	0.001, 0.000	−, 0.16
Minimum, maximum residual electron/density e Å^{-3}	−0.3, 0.6	−0.79, 1.02	−1.07, 0.90	−0.62, 0.82	−0.9, 0.79

[a] $R = \Sigma||F_o| - |F_c||/\Sigma|F_o|$. [b] $wR2 = [\Sigma w(F_o^2 - F_c^2)^2/\Sigma w(F_o^2)^2]^{\frac{1}{2}}$. [c] $R' = [\Sigma w(F_o^2 - F_c^2)^2/\Sigma w(F_o^2)^2]^{\frac{1}{2}}$. [d] $P = (F_o^2 + 2F_c^2)/3$.

mmol), tcne (0.061 g, 0.478 mmol) and L^4 (0.277 g, 0.478 mmol). Yield of yellow powder: 0.234 g (0.283 mmol, 65%). Crystals suitable for X-ray diffraction were grown by leading a gentle stream of N_2 through a solution in CH_2Cl_2. NMR ($CDCl_3$): ^{1}H, δ 2.17 (br s, 6 H, CH_3), 6.66 (2 H, aryl), 7.16–7.37 (22H, aryl) and 7.67 (apparent br d, 2H); ^{31}P-{^{1}H}, δ 6.26. IR (ν_{CN}, CH_2Cl_2): 2219 cm^{-1}. M.p. >573 K (decomposes, darkens upon heating).

[PdL^6(tcne)] 5. The complex [Pd(dba)$_2$] (0.200 g, 0.348 mmol), tcne (0.049 g, 0.383 mol) and L^6 (0.095 g, 0.383 mmol) were dissolved in toluene (30 cm^3). The reaction mixture was stirred for 1 h during which a yellow solution was formed. The solvent was concentrated to 3 cm^3 after which cold ether (30 cm^3) was added. The suspension formed was decanted and washed with cold ether (10 cm^3). The product was dried *in vacuo*. Yield of yellow powder: 0.151 g (0.31 mmol, 90%). Crystals suitable for X-ray diffraction were grown by slow diffusion of pentane in a solution of the product in CH_2Cl_2. NMR ($CDCl_3$): ^{1}H, δ 8.93, 8.80 [dd, 2 H, ^3J = 5.6, ^4J = 1.4, H(9), H(14)], 7.94, 7.87 [dt, 2 H, ^3J = 7.8, ^4J = 1.5, H(11), H(16)], 7.55, 7.52 [dd, 2 H, ^3J = 8.6, H(12), H(17)], 7.40, 7.34 [dd, 2 H, ^3J = 6.8 Hz, H(10), H(15)], 6.56 [dd, 1 H, ^3J = 5.5, 3.2, H(1)], 6.24 [dd, 1 H, ^3J = 5.5, 2.5, H(2)], 4.41 [d, 1 H, ^3J = 4.2, H(5)], 3.64 [s, 1 H, H(3)], 3.13 [dd, 1 H, ^3J = 3.9, H(4)], 3.48 [d, 1 H, ^3J = 1.4 Hz, H(6)], 1.90, 1.94 [m, 2 H, H(7)]; ^{13}C (230 K), δ 166.3, 165.1 [C(8), C(13)], 154.8, 151.9 [C(9), C(14)], 140.6, 139.3 [C(11), C(16)], 139.8, 136.7 [C(1), C(2)], 126.5, 124.4 [C(12), C(17)], 124.2, 122.4 [C(10), C(15)], 115.2, 114.6, 114.4, 114.1, (C=N), 54.6, 52.2, 46.9, 46.0 [C(3), C(6)], 47.1 [C(7)], 14.3, 14.0 (C=C). IR (ν_{CN}, KBr): 2224 cm^{-1} (Found: C, 56.6; H, 3.2; N, 16.95. Calc. for $C_{23}H_{16}N_6Pd$: C, 57.2; H, 3.35; N, 17.4%).

X-Ray crystallography

L^6. Data were collected on an Enraf-Nonius CAD-4 diffractometer (graphite monochromator) and ω–2θ scans. Crystal data and details of data collection and refinement are given in Table 7. Unit-cell parameters were refined by a least-squares fitting procedure using 23 reflections with 81 < 2θ < 88°. Corrections for Lorentz-polarisation effects were applied. The structure was solved by direct methods. The hydrogen-atom positions were calculated. Full-matrix least-squares refinement on F, anisotropic for the non-hydrogen atoms and isotropic for the hydrogen atoms, restraining the latter in such a way that the distance to their carrier remained constant at approximately 1.09 Å. The secondary isotropic extinction coefficient[57,58] refined to 0.23(3). Scattering factors were taken from Cromer and Mann.[59,60] All calculations were performed with XTAL,[61] unless stated otherwise.

Complexes 1, 2 and 4. Crystals suitable for X-ray determination were mounted on a Lindemann-glass capillary and transferred into the cold nitrogen stream on an Enraf-Nonius CAD4-T diffractometer with rotating anode (graphite mono-

chromator). Accurate lattice parameters were determined by least-squares treatment, using the setting angles (SET4) of about 25 reflections. The unit-cell parameters were checked for the presence of higher lattice symmetry.[61] Data were corrected for Lorentz-polarisation effects and for a linear decay of the three periodically measured reference reflections. The structures of compounds **1** and **2** were solved by automated direct methods (SIR 92),[63] **4** by automated Patterson methods and subsequent Fourier-difference techniques (DIRDIF 29).[64] Refinement on F^2 was carried out by full-matrix least-squares techniques (SHELXL 93).[65] Hydrogen atoms were included in the refinement in calculated positions riding on their carrier atoms. All non-hydrogen atoms were refined with anisotropic thermal parameters. The hydrogen atoms were refined with a fixed isotropic thermal parameter related to that of their carrier atom by a factor of 1.5 for the methyl hydrogen atoms and a factor of 1.2 for the others. Weights were optimised in the final refinement cycles. The unit cell of compound **1** contains one dichloromethane on an inversion centre for which no satisfactory disorder model could be refined. In a volume of 124 Å^3 an electron count of approximately 41 electrons was encountered and taken into the structure-factor calculation *via* back-Fourier transformation (PLATON/SQUEEZE).[66,67] Neutral atom scattering factors and anomalous dispersion corrections were taken from ref. 68.

Complex 5. Data were collected on an Enraf-Nonius CAD-4 diffractometer (graphite monochromator) and ω–2θ scans. Unit-cell parameters were refined by a least-squares fitting procedure using 23 reflections with $80 < 2\theta < 86°$. Corrections for Lorentz-polarisation effects were applied. The structure was solved and refined as for compound L^6. An empirical absorption correction (DIFABS[69]) was applied. The secondary isotropic extinction coefficient[57,58] refined to 0.02(1). Scattering factors were taken from Cromer and Mann.[59,60] The anomalous scattering of Pd was taken into account. All calculations were performed with XTAL,[61] unless stated otherwise.

Atomic coordinates, thermal parameters, and bond lengths and angles have been deposited at the Cambridge Crystallographic Data Centre (CCDC). See Instructions for Authors, *J. Chem. Soc., Dalton Trans.*, 1997, Issue 1. Any request to the CCDC for this material should quote the full literature citation and the reference number 186/477.

Acknowledgements

Dr. Petra Wehman is kindly acknowledged for stimulating discussions concerning palladium chemistry. We thank the Computational Chemistry List discussion group (http://ccl.osc.edu/chemistry.html) for helpful suggestions concerning π stacking in MOPAC. J. G. P. D. is indebted to Shell Research B.V. for financial support. This work was supported in part (A. L. S. and N. V.) by the Netherlands Foundation of Chemical Research (SON) with financial aid from the Netherlands Organisation for Scientific Research (NWO).

References

1 P. M. Maitlis, P. Espinet and M. J. H. Russell, in *Comprehensive Organometallic Chemistry*, eds. G. Wilkinson, F. G. A. Stone and E. W. Abel, Pergamon, Oxford, 1982, vol. 6, p. 233.
2 P. M. Maitlis, *The Organic Chemistry of Palladium*, Academic Press, New York, 1971, vol. 1, p. 106.
3 F. R. Hartley, in *Comprehensive Organometallic Chemistry*, eds. G. Wilkinson, F. G. A. Stone and E. W. Abel, Pergamon, Oxford, 1982, vol. 6, p. 471.
4 J. E. Bäckvall, in *Reactions of Coordinated Ligands*, ed. P. S. Braterman, Plenum, New York, 1986, vol. 1, p. 679.
5 *Chemistry of the Platinum Group Metals, Recent Developments*, ed. G. K. Anderson, Elsevier, Amsterdam, 1991.
6 J. Tsuji, *Organic Synthesis with Palladium Compounds*, Springer, Berlin, 1980.
7 C. A. Tolman, *Chem. Rev.*, 1977, **77**, 313.
8 C. G. Pierpont, R. M. Buchanan and H. H. Downs, *J. Organomet. Chem.*, 1977, **124**, 103.
9 R. van Asselt, C. J. Elsevier, W. J. J. Smeets and A. L. Spek, *Inorg. Chem.*, 1994, **33**, 1521.
10 H. Werner, G. T. Crisp, P. W. Jolly, H.-J. Kraus and C. Krüger, *Organometallics*, 1983, **2**, 1369.
11 V. V. Bashilov, P. V. Petrovskii, V. I. Sokolov, S. V. Lindeman, I. A. Guzey and Y. T. Struchkov, *Organometallics*, 1993, **12**, 991.
12 K. Okamoto, Y. Kai, N. Yasuoka and N. Kasai, *J. Organomet. Chem.*, 1974, **65**, 427.
13 M. Hodgson, D. Parker, R. J. Taylor and G. Ferguson, *J. Chem. Soc., Chem. Commun.*, 1987, 1309.
14 R. Benn, P. Betz, R. Goddard, P. W. Jolly, N. Kokel, C. Krüger and I. Topalovic, *Z. Naturforsch., Teil B*, 1991, **46**, 1395.
15 W. A. Hermann, W. R. Thiel, C. Broßmer, K. Öfele, T. Priermeier and W. Scherer, *J. Organomet. Chem.*, 1993, **461**, 51.
16 P. Hofmann, H. Heiß and G. Müller, *Z. Naturforsch., Teil B*, 1987, **42**, 395.
17 S. Sakaki and M. Ieki, *Inorg. Chem.*, 1991, **30**, 4218.
18 J. Li, G. Schreckenbach and T. Ziegler, *Inorg. Chem.*, 1995, **34**, 3245.
19 M. Kranenburg, Y. E. M. van der Burgt, P. C. J. Kamer, P. W. N. M. van Leeuwen, K. Goubitz and J. Fraanje, *Organometallics*, 1995, **14**, 3081.
20 U. Burkert and N. L. Allinger, *Molecular Mechanics*, American Chemical Society, Washington, D.C., 1982.
21 C. P. Casey and G. T. Whiteker, *Isr. J. Chem.*, 1990, **30**, 299.
22 C. P. Casey, G. T. Whiteker, M. G. Melville, L. M. Petrovich, J. J. A. Gavney and D. R. Powell, *J. Am. Chem. Soc.*, 1992, **114**, 5535.
23 M. Kranenburg, P. C. J. Kamer, P. W. N. M. van Leeuwen, D. Vogt and W. Keim, *J. Chem. Soc., Chem. Commun.*, 1995, 2177.
24 P. Wehman, H. M. A. van Dongen, A. Hagos, P. C. J. Kamer and P. W. N. M. van Leeuwen, unpublished work.
25 J. M. Brown and P. J. Guiry, *Inorg. Chim. Acta*, 1994, **220**, 249.
26 R. E. Rülke, P. W. N. M. van Leeuwen and K. Vrieze, unpublished work.
27 M. Kranenburg, P. C. J. Kamer and P. W. N. M. van Leeuwen, unpublished work.
28 J. J. P. Stewart, MOPAC, Program 455, Quantum Chemistry Program Exchange, Indiana University, IN, 1990.
29 M. J. S. Dewar, E. G. Zhoebisch, E. F. Healy and J. J. P. Stewart, *J. Am. Chem. Soc.*, 1985, **107**, 3902.
30 J. J. P. Stewart, *J. Comput. Chem.*, 1989, **10**, 209.
31 M. J. S. Dewar and W. Thiel, *J. Am. Chem. Soc.*, 1977, **99**, 4899.
32 A. Buhling, J. W. Elgersma, K. Goubitz, J. Fraanje, P. C. J. Kamer and P. W. N. M. van Leeuwen, unpublished work.
33 O. A. D'yachenko, Y. A. Sokolova and L. O. Atovmyan, *Zh. Strukt. Khim.*, 1984, **25**, 83.
34 C. A. Hunter and J. K. M. Sanders, *J. Am. Chem. Soc.*, 1990, **112**, 5525.
35 M. D. Gordon, T. Fukunaga and H. E. Simmons, *J. Am. Chem. Soc.*, 1976, **98**, 8401.
36 T. Bally, *Faraday Discuss. R. Soc. Chem.*, 1994, **90**, 1799.
37 J. J. P. Stewart, personal communication.
38 Y. Kurita, C. Takayama and S. Tanaka, *J. Comput. Chem.*, 1994, **15**, 1013.
39 J. Perlstein, *J. Am. Chem. Soc.*, 1994, **116**, 11 420.
40 M. J. S. Dewar and C. Jie, *Theochem*, 1989, **56**, 1.
41 C. K. Johnson, ORTEP, Report ORNL-5138, Oak Ridge National Laboratory, Oak Ridge, TN, 1976.
42 S. D. Ittel and J. A. Ibers, *Adv. Organomet. Chem.*, 1976, **14**, 33; K. S. Wheelock, J. H. Nelson, L. C. Cusachs and H. B. Jonassen, *J. Am. Chem. Soc.* 1970, **92**, 5110; J. H. Nelson and H. B. Jonassen, *Coord. Chem. Rev.*, 1971, **6**, 27.
43 V. P. Zagorodnikov, S. B. Katser, M. N. Vargaftik, M. A. Porai-Koshits and I. I. Moiseev, *J. Coord. Chem.*, 1989, **15**, 1540.
44 R. A. Klein, R. van Belzen, C. J. Elsevier and K. Goubitz, unpublished work.
45 K. Tatsumi, R. Hoffmann, A. Yamamoto and J. K. Stille, *Bull. Chem. Soc. Jpn.*, 1981, **54**, 1857.
46 P.-T. Cheng, C. D. Cook, C. H. Koo, S. C. Nyburg and M. T. Shiomi, *Acta Crystallogr., Sect. B*, 1971, **27**, 1904.
47 G. Bombieri, E. Forsellini, C. Panattoni, R. Graziani and G. Bandoli, *J. Chem. Soc. A*, 1970, 1313.
48 J. N. Francis, A. McAdam and J. A. Ibers, *J. Organomet. Chem.*, 1971, **29**, 131.
49 P.-T. Cheng and S. C. Nyburg, *Can. J. Chem.*, 1972, **50**, 912.
50 CAChe WorkSystem, version 3.7, CAChe Scientific Inc., Beaverton, OR, 1994.
51 M. J. S. Dewar and Y.-C. Yuan, *Inorg. Chem.*, 1990, **29**, 3881.
52 M. J. S. Dewar, *Organometallics*, 1987, **6**, 1486.

53 M. J. S. Dewar, M. L. McKee and H. S. Rzepa, *J. Am. Chem. Soc.*, 1978, **100**, 3607.
54 M. J. S. Dewar, J. Friedheim, G. Grady, E. F. Healy and J. J. P. Stewart, *Organometallics*, 1986, **5**, 375.
55 M. J. S. Dewar and C. H. Reynolds, *J. Comput. Chem.*, 1986, **7**, 140.
56 M. F. Rettig and P. M. Maitlis, *Inorg. Synth.*, 1977, **17**, 134.
57 W. H. Zachariasen, *Acta Crystallogr., Sect. A*, 1967, **23**, 558.
58 A. C. Larson, in *Crystallographic Computing*, eds. F. R. Ahmed, S. R. Hall and C. P. Huber, Munksgaard, Copenhagen, 1969, p. 291.
59 D. T. Cromer and J. B. Mann, *Acta Crystallogr., Sect. A*, 1968, **24**, 321.
60 *International Tables for X-Ray Crystallography*, Kynoch Press, Birmingham, 1974, vol. 4, p. 55.
61 *XTAL 3.2 Reference Manual*, eds. S. R. Hall, H. D. Flack and J. M. Stewart, Universities of Western Australia, Geneva and Maryland, 1992.
62 A. L. Spek, *J. Appl. Crystallogr.*, 1988, **21**, 578.
63 A. Altomare, G. Cascarano, C. Giacovazzo and A. Guagliardi, *J. Appl. Crystallogr.*, 1993, **26**, 343.
64 P. T. Beurskens, G. Admiraal, G. Beurskens, W. P. Bosman, S. García-Granda, R. O. Gould, J. M. M. Smits and C. Smykalla, The DIRDIF program system; Technical report of the Crystallography Laboratory, University of Nijmegen, 1992.
65 G. M. Sheldrick, SHELXL 93, Program for crystal structure refinement, University of Göttingen, 1993.
66 A. L. Spek, *Acta Crystallogr., Sect. A*, 1990, **46**, C34.
67 A. L. Spek, *ACA Abstr.*, 1994, **22**, 66.
68 *International Tables for Crystallography*, ed. A. J. C. Wilson, Kluwer, Dordrecht, 1992, vol. C.
69 N. Walker and D. Stuart, *Acta Crystallogr., Sect. A*, 1983, **39**, 158.

Received 21*st November* 1996; *Paper* 6/07927J